

Mapping W R 140 from infrared spectroscopy and imaging

P. M. Williams

Institute of Astronomy, Royal Observatory, Edinburgh, EH 9 3HJ, U.K.

W. P. Varricatt

Joint Astronomy Centre, 660 N. A'ohoku Place, Hilo, HI 96720, U.S.A.

A. P. Marston

European Space Research and Technology Center (ESTEC), European Space Agency, Keplerlaan 1, AG NL-2200 Noordwijk, Netherlands

N. M. Ashok

Physical Research Laboratory, Navrangpura, Ahmedabad, India 380009

Abstract. Observations of the 1.083- μ m He I line in W R 140 (HD 193793) show P-Cygni profiles which varied as the binary system went through periastron passage. A sub-peak appeared on the normally at-topped emission component and then moved across the profile consistent with its formation in the wind-collision region. Variation of the absorption component provided constraints on the opening angle (θ) of the wind-collision region. Infrared (2-10- μ m) images observed with a variety of instruments in 2001-04 resolve the dust cloud formed in 2001, and show it to be expanding at a constant rate. Owing to the high eccentricity of the binary orbit, the dust is spread around the orbital plane in a 'splash' and we compare the dust images with the orientation of the orbit.

1. Infrared spectroscopy and the 1.083- μ m He I P-Cygni profile

The WC7+O4-5 binary W R 140 (HD 193793) is the archetypal episodic dust-forming Wolf-Rayet Colliding Wind Binary. It is particularly luminous in X-rays and was the first WR system to show non-thermal radio emission and episodic dust formation. Variations in its X-ray, radio and infrared properties were linked to its binary motion by Williams et al. (1990), and it has since been the subject of theoretical and observational studies of colliding-wind phenomena. As part of the campaign planned for the 2001 periastron passage, we observed a series of near-infrared spectra having resolutions $R \sim 1000$ using the United Kingdom Infrared Telescope (UKIRT), Hawaii, and the Mt Abu Infrared Telescope, India (Varricatt, Williams & Ashok 2004). The 1.083- μ m He I line was also observed at $R \sim 4700$ to look for colliding-wind effects (cf. Stevens & Howarth 1999). Previous observations of W R 140 (e.g. Eenens & Williams 1994) had shown at-topped profiles for this line, but they were taken far from periastron. Our observation at $\phi = 0.96$, however, showed the appearance of a strong, blue-shifted sub-peak on the emission profile (Fig.1), which we interpret as being

formed in a shell of compressed WC7 stellar wind material flowing along the wind-collision region (WCR). The shape of the WCR can be approximated (e.g. Usov 1992., Luhrs 1996) by a hollow cone symmetric about the axis joining the stars and having its apex towards the WC7 star, which has the higher mass-loss rate.

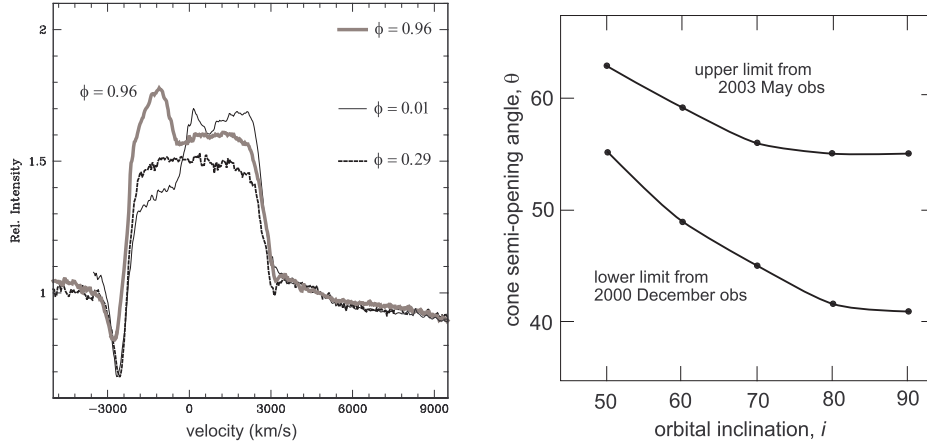


Figure 1. Left: profiles of the 1.083- μ m He I line in 2000 October ($\phi = 0.96$), 2001 March ($\phi = 0.01$) and 2003 ($\phi = 0.29$), which is typical of most of the orbit). Right: constraints on the opening angle (θ) of the wind-collision region as a function of orbital inclination set by the varying strength of the absorption component of the He I line.

At $\phi = 0.96$, the system is near conjunction with the O star in front of the WC7 star, so we expect the compressed WC7 material to be flowing towards us. At the same time, we are viewing the two stars mostly through the wind of the O star, accounting for our observation (Fig. 1) that the absorption component of the He I line is weaker than at phases when the stars are observed through the Herich WC7 stellar wind. At this phase, the angle between our sightline and the axis joining the two stars is smaller than the opening angle (θ) of the wind-collision 'cone'.

The value of θ varies round the orbit and can be calculated for the phases of our observations for a range of values of the inclination so we can use successive measurements of the strength of the absorption component to explore permitted values of θ and inclination. At the same time, we model the variation of the radial velocity (RV) of the subpeak, including its width, following Luhrs (1997) but with the difference that, instead of treating the velocity of the compressed wind as a free parameter to be fit, we calculate it from those of the WC7 and O star winds and following Canto, Raga & Wilkins (1996). This models the movement of the sub-peak to the red end of the profile by the time of our first post-periastron observation ($\phi = 0.01$, Fig. 1). At this time, the absorption component was strong because we observed both stars through the WC7 stellar wind. Two years later, by $\phi = 0.29$, the emission sub-peak had vanished as the stars had moved further apart, but the absorption component was still strong. This puts a useful upper limit on θ (Fig. 1). Modelling the RVs of the sub-peak indicates an orbital inclination $i \approx 65^\circ \pm 10^\circ$, implying (Fig. 1) $\theta \approx 53^\circ \pm 10^\circ$.

2. Infrared imaging of the dust emission

We imaged W R 140 in the infrared with four different instruments: PHARO + AO on the Hale telescope, INGRID + AO (NAOMI) on the William Herschel Telescope (WHT), and UIST and Michelle, both on UKIRT. The UKIRT observations were made at longer wavelengths, where the contrast between dust and stellar emission was greater, especially as the dust cooled, but the resolution is lower. Single stars were observed to determine the image psfs and the images of W R 140 were restored using maximum entropy methods. A test of the validity of our procedures is provided by two images of W R 140 (Fig. 2) observed at about the same time with two different instruments and reduced with different software packages. The basic structures are similar, with a bar of dust emission to the south and another feature to the east. Similar structures are evident in all the images, e.g. a 3.99- μ m image observed with UIST in 2003 (Fig. 3).

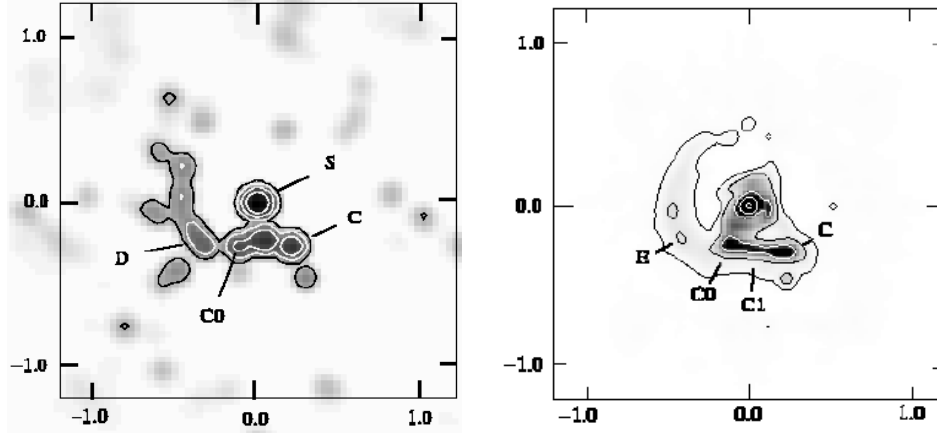


Figure 2. Two 2- μ m images of W R 140 observed in 2002 July with different instruments: NAOMI/INGRID on the WHT (left) and AO/PHARO system on the Hale (right). Both images have NE at top left and the scale is arcsec from the central star (S). Dust emission knots (C', D' and E') correspond to those identified in the 2001 images of Monnier et al. (2002).

We can use the contemporaneous 3.6- μ m and 3.99- μ m UIST observations to measure the infrared colours of the emission features relative to that of the star, confirming that the features are 0.4 mag. redder in [3.6]/[3.99] than the star, consistent with their being heated dust. We identified several knots of dust emission with those identified in the aperture-masking images observed in 2001 by Monnier, Tuthill & Danchi (2002) from the similarity of their position angles (P.A.) relative to the star, and use these and other knots to track the expansion of the dust cloud. The observations are summarized in Table 1, together with the P.A.s and radial distances (r) of the emission knot, C'. These distances, together with those from the images of Monnier et al. and measured from the image given by Tuthill et al. (2003), and similar data for knot E' to the east, are plotted against date in Fig. 3, and show remarkably linear expansion.

The proper motions of selected knots from linear fits to the distances of selected knots are given in Table 2, together with projected velocities adopting

Table 1. Log of imaging observations of W R 140 with position angle and distance of dust emission knot C' from the star

Instrument	Date	Phase	Scale (mas)	obs (m)	P.A. ($^{\circ}$)	r (mas)
Hale: PHARO + AO	2001.68	0.073	25	2.2		
Hale: PHARO + AO	2002.31	0.153	25	2.2	216	278
WHT: INGRID + AO	2002.51	0.178	26.3	2.27	219	341
Hale: PHARO + AO	2002.56	0.184	25	2.2	217	352
UKIRT: UIST	2002.89	0.226	16.5	3.6	217	498
UKIRT: UIST	2002.89	0.226	16.5	3.99	216	451
UKIRT: UIST	2003.42	0.293	16.5	3.6	210	630
UKIRT: UIST	2003.42	0.293	16.5	3.99	217	601
UKIRT: Michelle	2004.25	0.397	210	10.52	215	874
UKIRT: UIST	2004.49	0.426	16.5	3.99	214	948
UKIRT: UIST	2004.49	0.426	16.5	4.68	218	928

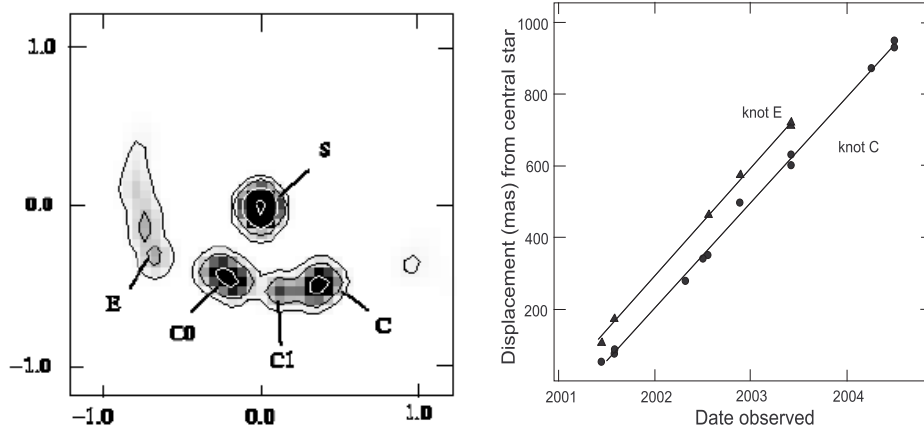


Figure 3. Left: A 3.99- μ m image of W R 140 observed on 2003 June 4 with UIST on UKIRT showing homologous expansion of the dust emission features observed in earlier images. The resolution is lower than in Fig. 2 owing to the longer wavelength. Right: proper motions of knots C' and E' of dust emission measured from our images and the 2001 images of Monnier et al. and Tuthill et al. (2003).

the revised distance of 1.85 kpc (Dougherty et al., this meeting). These velocities are comparable to that (2470 km/s) of the compressed WC7 wind material responsible for the He I sub-peaks and presumably the gas in which the dust formed. The observation of relatively high projected velocities for three of the four well observed knots suggests either that they are clumps moving in the plane of the sky or, more probably, that they are limb-brightened edges of a hollow dust cloud and not physical clumps.

To model the dust emission images, we assume that the dust moves radially along the projection of the WC7 and therefore need to know the changing configuration of the WC7 during dust formation. From the NIR light curves

Table 2. Proper motions, projected velocities and ejection dates of dust-emission knots^a.

Knot	P.M. (mas/y)	Proj. vel. (km/s)	Date started	Phase started
C	294 7	2575 63	2001.28 0.07	0.023 0.009
C0	240 17	2108 151	2001.34 0.21	0.030 0.027
D	313 18	2745 158	2001.22 0.11	0.015 0.014
E	304 2	2664 14	2001.03 0.01	0.991 0.002

(William s 1990), we infer that dust formation occurs for only 2–3% of the period on either side of periastron. The high eccentricity of the orbit (M archenko et al. 2003), however, means that the axis of the W CR moves through more than 180° in this short time and, allowing for $\theta = 53^\circ$, that the dust is spread around three-quarters of the orbital plane in a small fraction of the period. This will not give a dust ‘spiral’, nor a ‘jet’, but a ‘splash’. The orientation of this ‘splash’ on the sky using the orientation of the orbit from values of θ and i derived by Dougherty et al. has the dust starting to the east and running clockwise round the star to finish to the south, making the southern ‘bar’ the most recently formed dust. The absence of significant dust emission to the NW, the projected axis at the time of periastron passage, suggests that dust formation is quenched at the very closest separation.

Acknowledgements. We gratefully acknowledge the Service Observing Programme of the Isaac Newton Group (WHT) and the Joint Astronomy Centre (UKIRT).

References

- Canto J., Raga A.C., Wilkin F.P., 1996, *ApJ*, 469, 729
 Eenens P.R.J., Williams P.M., 1994, *MNRAS*, 269, 1082
 Luhrs S., 1997, *PASP*, 109, 504
 M archenko S.V., Mot A.F.J., Ballereau D., Chauville J., Zorec J., Hill G.M., Annuk K., Corral L.J., Demers H., Eenens P.R.J., Panov K.P., Seggewiss W., Thomson J.R., Villar-Sba A., 2003, *ApJ*, 596, 1295
 Monnier J.D., Tuthill P.G., Danchi W.C., 2002, *ApJ*, 567, L137
 Stevens I.R., Howarth, I.D., 1999, *MNRAS*, 302, 549
 Tuthill P.G., Monnier J.D., Danchi, W.C., Turner N.H., 2003, in *IAU Symp.* 212, *A Massive Star Odyssey, from Main Sequence to Supernova*, ed. K.A. van der Hucht, A. Herrero & C. Esteban (San Francisco: ASP), 121
 Usov V.V., 1992, *ApJ*, 389, 635
 Varricatt W.P., Williams P.M., Ashok N.M., 2004, *MNRAS*, 351, 1307
 Williams P.M., van der Hucht K.A., Pollock A.M.T., Florkowski D.R., van der Woerd H., Wamstecker W.M., 1990, *MNRAS*, 243, 662